Exact BER Analysis of DS-UWB Multiple Access Systems in Lognormal Multipath Fading Channels

Wei Cao, A. Nallanathan and Chin Choy Chai

Abstract

In this paper, exact BER analysis is carried out using the Characteristic Function (CF) method for DS UWB systems in lognormal multipath fading channels. Unlike the Gaussian Approximation (GA) method, the CF method deals with exact probability distribution function (PDF) of the total noise (including multiple access interference (MAI), self interference (SI) and AWGN) instead of making approximation on PDF of the total noise. Exact BER formula is derived and verified by simulation results. It is shown that the CF method is more accurate than the GA method in BER calculation when SNR is large. Based on the BER formula, performance of the DS PAM UWB and DS PPM UWB systems is accurately compared. Discussions based on characteristic functions provide further insight into the numerical results.

Index Terms

Direct sequence, ultra wideband, multiple access interference, bit error rate, lognormal multipath fading channels

Wei Cao and A. Nallanathan are with the Electrical and Computer Engineering Department, National University of Singapore. (Email: caowei@nus.edu.sg, elena@nus.edu.sg). Chin Choy Chai is with Institute for Infocomm Research, Singapore. (Email: chaicc@i2r.a-star.edu.sg)

I. Introduction

Time hopping (TH) and direct sequence (DS) are the most popular multiple access methods that are combined with ultra-wide band (UWB) impulse radio (IR) systems. TH was originally proposed for multiple access UWB systems in [1]. Later DS has been investigated as an alternative multiple access method for UWB systems [2] - [4]. Combination of TH and DS multiple access has also been proposed recently [5]. TH UWB systems use user “signature” of hopping code in time domain and extend symbol duration, while DS UWB systems use pseudo-random ± 1 spreading codes to provide multiple access capability and generally have much smaller symbol duration. Therefore, TH UWB is suitable for low data rate applications, while DS UWB can support high data rate applications. Since symbols are transmitted by dense pulse train in DS UWB systems, multiple access interference (MAI) becomes a main limitation to system performance with the growth of number of users. Commonly used modulation methods in UWB communications are pulse position modulation (PPM)[1] and pulse amplitude modulation (PAM). Combination of PPM and PAM was also proposed for UWB systems in [6].

Theoretical calculation of bit error rate (BER) for various UWB systems has been discussed in numerous literature. Most of earlier works focused on TH UWB systems, for example [1], [7] - [9]. Later theoretical evaluation of BER for DS UWB multiple access systems was reported in several literature [10] - [13]. The BER analysis methods used in these literature can be grouped into two categories. The first is called the Gaussian Approximation (GA) method, including standard GA, improved GA and some variants. The GA methods are based on the Central Limit Theorem (CLT) and assume that interference terms are Gaussian random variables. The second is named as the Characteristic Function (CF) method, which performs interference analysis without any assumption on interference distribution. Generally the CF method yields more accurate BER evaluation than the GA method at the expense of higher computational complexity.

The GA method is widely used for UWB systems performance analysis: In [1], multiple access

[1] In early research on UWB communications, PPM was almost exclusively adopted since negative UWB pulses were difficult to implement. Lately, generating negative pulses becomes easier and PAM attracts more attention.

performance of TH PPM UWB systems under perfect power control in AWGN channels was considered. Multiple access performance of UWB systems using pseudo-chaotic TH code was studied in [7]. In [10], performance of DS BPSK UWB systems with large number of users was evaluated under both perfect and imperfect power control. Performance of TH UWB and DS IR UWB multiple access systems was investigated and compared in [5]. Though the GA method is simple to apply in AWGN channels, its validity is questionable as reported in [14].

Using the GA method, the resultant BER formula in AWGN channels has a closed form (erfc function). However, BER analysis in fading channels is not so easy: the probability density function (PDF) of instantaneous output SINR is needed if the GA method is to be used in multipath fading channels. Generally numerical averaging (so-called semi-analytical/simulation approach) is needed to assist the GA method to obtain the average BER. Thus the GA method losses its main advantages: simplicity and closed form formula. A BER lower bound of TH UWB systems in multipath Rayleigh fading channels was presented in [8] under GA assumption. In [11], the conditional BER of DS BPSK UWB systems was derived in multipath channels with narrow band interference, and the average BER was obtained by numerical averaging. In [12], the GA method is used to evaluate BER of DS PPM UWB systems under perfect power control in a simplified lognormal multipath fading channel, where averaging on fading channels is also needed to obtain average BER values.

Though the CF method has been used for exact BER analysis of both TH UWB and DS UWB systems, all previous works were done in AWGN channels only. Unlike the GA method, the CF method does not make approximation on the distribution of interference. It makes use of real distribution of the total noise, including interference and AWGN, to compute exact BER values. BER evaluation based on the CF method for TH UWB systems was carried out in [9]. Exact BER performance of DS BPSK UWB and DS PPM UWB multiple access systems was studied in [15] and [16] respectively. The results in all these works show that the CF method evaluates BER exactly, while the GA method significantly underestimates BER in medium and large SNR range. Exact BER performance evaluation of UWB systems in AWGN channels shows the power of the CF method and verifies that the GA method is not so suitable for BER calculation of UWB systems.

In this paper, we apply the CF method to calculate exact BER values of DS PAM UWB and DS PPM UWB multiple access systems in a more practical lognormal multipath fading channel. Exact BER formula is derived, which can be used to provide useful performance evaluation for various UWB applications. Simulation results show that the CF method is more accurate than the GA method in BER calculation. Performance of DS PAM UWB and DS PPM UWB systems is accurately compared using the BER formula derived. Furthermore, discussions based on characteristic function provide more insight into the numerical results.

II. System and Channel Models

DS PAM UWB and DS PPM UWB systems use the same multiple access scheme but different modulation techniques. Description of these two systems can be found in our previous works [15][16]. Here these two systems are expressed in a unified framework to facilitate BER derivation and performance comparison.

A. Signal Format

The analytical expressions of DS PAM UWB and DS PPM UWB signals are given below.

$$\begin{aligned} s_{PAM}^{(k)}(t) &= \sqrt{P} \sum_{i=-\infty}^{\infty} b_i^k \sum_{n=0}^{N_r-1} a_n^k z(t - iT_r - nT_c) \\ s_{PPM}^{(k)}(t) &= \sqrt{P} \sum_{i=-\infty}^{\infty} \sum_{n=0}^{N_r-1} a_n^k z(t - 2iT_r - nT_c - b_i^k T_p) \end{aligned} \tag{1}$$

where k is the index of user, i is the index of symbol and $z(t)$ represents the energy normalized UWB monocycle with duration of T_p. Other parameters are explained as follows.

1) P is the transmitted signal power of each user.
2) $\{b_i^k\}_{i=-\infty}^{\infty}$ represents data symbol sequence of the k^{th} user. $b_i^k \in \{-1, +1\}$ in the DS binary PAM UWB system, while $b_i^k \in \{0, 1\}$ in the DS binary PPM UWB system. In both systems, b_i^k takes two possible values with equal probability.
3) N_r is the number of chips in one symbol. In each chip, there is one and only one UWB monocycle.

4) $\{a_n^k\}_{n=0}^{N_r-1}$ is the DS code of the k^{th} user. Random DS code is assumed, i.e., for every $n = \{0, 1, \cdots, N_r - 1\}$ and $k = \{0, 1, \cdots, K-1\}$, $a_n^k \in \{-1, +1\}$ with equal probability.
5) T_c is the chip duration and T_r is the symbol duration, i.e., $T_r = N_r T_c$.
6) The time shift associated with PPM is T_p in the orthogonal binary PPM signal set, which equals to the duration of $z(t)$. Furthermore, we set $T_p = T_c/4$ so that time shift associated with PPM is smaller than the chip duration.
7) In the DS PPM UWB system, a guarding interval T_r is inserted to avoid inter-symbol interference (ISI), where T_r is assumed to be greater than the maximal delay spread of the channel.

B. UWB Channel Model

According to [17], channel impulse response of the k^{th} user is modeled as

$$h^{(k)}(t) = \sum_{l=0}^{L-1} \alpha_{k,l} \delta(t - \tau_{k,l}) \tag{2}$$

where L is the number of multipaths, $\alpha_{k,l}$ represents the l^{th} path gain and $\tau_{k,l}$ is the l^{th} path delay.

We consider an analytically feasible channel model with resolvable multipaths [6][11], i.e., $\tau_{k,l} = \tau_{k,0} + lT_c$. Since multipath components tend to arrive in clusters, the l^{th} path can be expressed as the j^{th} ray in the i^{th} cluster. Therefore, delay of the l^{th} path can be rewritten as $\tau_{k,l} = \mu_{k,i} + \nu_{k,j,i}$, where $\mu_{k,i}$ is delay of the i^{th} cluster and $\nu_{k,j,i}$ is delay of the j^{th} ray in the i^{th} cluster relative to $\mu_{k,i}$.

Path gain $\alpha_{k,l}$ is decomposed as $\alpha_{k,l} = \theta_{k,l}\beta_{k,l}$, where $\theta_{k,l} \in \{\pm 1\}$ represents the random phase due to reflection, $\beta_{k,l}$ is the lognormal fading amplitude with following PDF.

$$p_{\beta_{k,l}}(\beta_{k,l}) = \frac{20 \exp\left(-\frac{(20\log_{10}\beta_{k,l} - \eta_{k,l})^2}{2\varrho_{k,l}^2}\right)}{\beta_{k,l}\sqrt{2\pi\varrho_{k,l}^2}\ln 10} \tag{3}$$

where $\eta_{k,l}$ and $\varrho_{k,l}^2$ are mean and variance of a Gaussian random variable $y_{k,l}$ ($y_{k,l} = 20\log_{10}\beta_{k,l}$) respectively.

The power delay profile of the channel is double exponential decaying by rays and clusters, i.e., $\mathrm{E}\left[\beta_{k,l}^2\right] = \Omega_0 \exp(-\mu_{k,i}/\Gamma)\exp(-\nu_{k,j,i}/\gamma)$, where Ω_0 is the mean energy of the 0^{th} ray in the 0^{th} cluster. Γ and γ represent the cluster decay factor and ray decay factor respectively. The channel is normalized to have unit energy, i.e., $\sum_{l=0}^{L-1} \mathrm{E}\left[\beta_{k,l}^2\right] = 1$. Since transmitters and receivers are stationary in most WPAN applications [17], the channel is assumed to remain constant over a block of symbols.

C. Received Signal

Received signal $r_{PAM/PPM}(t)$ is given by

$$r_{PAM/PPM}(t) = \sum_{k=0}^{K-1} \sum_{l=0}^{L-1} \alpha_{k,l} s_{PAM/PPM}^{(k)}(t - \tau_k - lT_c) + n(t) \tag{4}$$

where τ_k is asynchronous transmission delay of the k^{th} user uniformly distributed over $[0, T_r)$, $n(t)$ is AWGN with double sided power spectral density of $N_0/2$.

Template waveforms used in the correlator receiver of the k^{th} user are given as follows.

$$\begin{aligned} v_{PAM}^{(k)}(t) &= \alpha_{k,0} \sum_{n=0}^{N_r-1} a_n^k z(t - nT_c) \\ v_{PPM}^{(k)}(t) &= \alpha_{k,0} \sum_{n=0}^{N_r-1} a_n^k q(t - nT_c) \end{aligned} \tag{5}$$

where $q(t) = z(t) - z(t - T_p)$ is the template waveform for the orthogonal binary PPM signal set.

III. Characteristic Function Analysis of DS PAM UWB System

A. Decision Statistics

The 0^{th} user is assumed to be the desired user with perfect synchronization, i.e. $\tau_0 = 0$ in (4). The 0^{th} receiver captures the 0^{th} path, where $\alpha_{k,0}$ is known at the receiver.

The output decision statistic Z_{PAM} from the 0^{th} receiver is given by

$$\begin{aligned} Z_{PAM} &= \int_0^{T_r} r_{PAM}(t) v_{PAM}^{(0)}(t) dt \\ &= \underbrace{\int_0^{T_r} \alpha_{0,0} s_{PAM}^{(0)}(t) v_{PAM}^{(0)}(t) dt}_{Z_{PAM}^{(0)}} + \underbrace{\int_0^{T_r} \sum_{l=1}^{L-1} \alpha_{0,l} s_{PAM}^{(0)}(t - lT_c) v_{PAM}^{(0)}(t) dt}_{I_{PAM}} \\ &\quad + \underbrace{\int_0^{T_r} \sum_{k=1}^{K-1} \sum_{l=0}^{L-1} \alpha_{k,l} s_{PAM}^{(k)}(t - \tau_k - lT_c) v_{PAM}^{(0)}(t) dt}_{M_{PAM}} + \underbrace{\int_0^{T_r} n(t) v_{PAM}^{(0)}(t) dt}_{N_{PAM}} \end{aligned} \tag{6}$$

where $Z_{PAM}^{(0)}$ is the desired signal, I_{PAM} is the self interference (SI) caused by multipath propagation, M_{PAM} is the MAI and N_{PAM} is the AWGN.

A.1. Desired Signal

$Z_{PAM}^{(0)}$ is the contribution from the 0^{th} path of the 0^{th} user.

$$Z_{PAM}^{(0)} = \int_0^{T_r} \alpha_{0,0} s_{PAM}^{(0)}(t) \alpha_{0,0} \sum_{n=0}^{N_r-1} a_n^0 z(t - nT_c) dt = \alpha_{0,0}^2 b_0^0 \sqrt{P} N_r \tag{7}$$

A.2. Multiple Access Interference

M_{PAM} is the sum of signal from $K-1$ interfering users, which consists of $(K-1) \times L$ terms.

$$M_{PAM} = \sum_{k=1}^{K-1} \sum_{l=0}^{L-1} \underbrace{\int_0^{T_r} \alpha_{k,l} s_{PAM}^{(k)}(t - \tau_k - lT_c) \alpha_{0,0} \sum_{n=0}^{N_r-1} a_n^0 z(t - nT_c) dt}_{M_{PAM}^{(k,l)}} \tag{8}$$

Contribution of the l^{th} path of the k^{th} user, $M_{PAM}^{(k,l)}$, is modeled as

$$\begin{aligned} M_{PAM}^{(k,l)} &= \int_0^{T_r} \alpha_{k,l} s_{PAM}^{(k)}(t - \tau_k - lT_c) \alpha_{0,0} \sum_{n=0}^{N_r-1} a_n^0 z(t - nT_c) dt \\ &= \alpha_{0,0} \alpha_{k,l} \sqrt{P} \left[R_{PAM}(\Delta T_k) X_{PAM}^{(k,l)} + \hat{R}_{PAM}(\Delta T_k) Y_{PAM}^{(k,l)} \right] \end{aligned} \tag{9}$$

where we introduce following ancillary definitions.

1) τ_k, the asynchronous transmission delay, is split into two parts: an integer multiple of T_c and a remaining part ΔT_k.

$$\tau_k = \gamma_k T_c + \Delta T_k \tag{10}$$

where $\gamma_k \in \{0, 1, \cdots, N_r - 1\}$ and $\Delta T_k \in [0, T_c)$, both with uniform distribution in their respective domains.

2) $R_{PAM}(\Delta T_k)$ and $\hat{R}_{PAM}(\Delta T_k)$ are defined as the autocorrelation functions of $z(t)$. Generally $z(t)$ is symmetrical and $R_{PAM}(\Delta T_k) = \hat{R}_{PAM}(T_c - \Delta T_k)$.

$$\begin{aligned} R_{PAM}(\Delta T_k) &= \int_0^{\Delta T_k} z(t) z(t + T_c - \Delta T_k) dt \\ \hat{R}_{PAM}(\Delta T_k) &= \int_{\Delta T_k}^{T_c} z(t) z(t - \Delta T_k) dt \end{aligned} \tag{11}$$

3) $X_{PAM}^{(k,l)}$ and $Y_{PAM}^{(k,l)}$ are defined as follows.

$$\begin{aligned} X_{PAM}^{(k,l)} &= b_{-1}^{k} \sum_{n=0}^{\gamma_k+l} a_n^0 a_{n+N_r-\gamma_k-l-1}^{k} + b_0^k \sum_{n=\gamma_k+l+1}^{N_r-1} a_n^0 a_{n-\gamma_k-l-1}^{k} \\ Y_{PAM}^{(k,l)} &= b_{-1}^{k} \sum_{n=0}^{\gamma_k+l-1} a_n^0 a_{n+N_r-\gamma_k-l}^{k} + b_0^k \sum_{n=\gamma_k+l}^{N_r-1} a_n^0 a_{n-\gamma_k-l}^{k} \end{aligned} \tag{12}$$

It can be proved [18, Chapter 4, Eq. (4-55) to (4-56)] that for all different k and l, $X_{PAM}^{(k,l)}$ and $Y_{PAM}^{(k,l)}$ are independent and identical Binomial random variables due to random property of b_i^k and a_n^k. The distribution of $X_{PAM}^{(k,l)}$ and $Y_{PAM}^{(k,l)}$ is given by

$$P(X=x) = \begin{pmatrix} N_r \\ \frac{x+N_r}{2} \end{pmatrix} \frac{1}{2^{N_r}} \tag{13}$$

where the range of X (or $X_{PAM}^{(k,l)}$, $Y_{PAM}^{(k,l)}$) is $\{-N_r, -N_r+2, \cdots, N_r-2, N_r\}$.

According to (8) and (9), interference from the k^{th} user, $M_{PAM}^{(k)}$, is given by

$$M_{PAM}^{(k)} = \sum_{l=0}^{L-1} M_{PAM}^{(k,l)} = \alpha_{0,0}\sqrt{P}\left[R_{PAM}(\Delta T_k)\sum_{l=0}^{L-1}\alpha_{k,l}X_{PAM}^{(k,l)} + \hat{R}_{PAM}(\Delta T_k)\sum_{l=0}^{L-1}\alpha_{k,l}Y_{PAM}^{(k,l)}\right] \tag{14}$$

A.3. Self Interference

SI from the l^{th} path, $I_{PAM}^{(l)}$, is modeled as

$$\begin{aligned} I_{PAM}^{(l)} &= \int_0^{T_r} \alpha_{0,l} s_{PAM}^{(0)}(t-lT_c)\alpha_{0,0}\sum_{n=0}^{N_r-1} a_n^0 z(t-nT_c)dt \\ &= \alpha_{0,0}\alpha_{0,l}\sqrt{P}[R_{PAM}(0)X_{PAM}^{(0,l)} + \hat{R}_{PAM}(0)Y_{PAM}^{(0,l)}] \\ &= \alpha_{0,0}\alpha_{0,l}\sqrt{P}Y_{PAM}^{(0,l)} \end{aligned} \tag{15}$$

And I_{PAM} is given by

$$I_{PAM} = \sum_{l=1}^{L-1} I_{PAM}^{(l)} = \alpha_{0,0}\sqrt{P}\sum_{l=1}^{L-1}\alpha_{0,l}Y_{PAM}^{(0,l)} \tag{16}$$

A.4. AWGN

N_{PAM} in (6) is expressed as

$$N_{PAM} = \int_0^{T_r} n(t)\alpha_{0,0} \sum_{n=0}^{N_r-1} a_n^0 z(t - nT_c)dt \tag{17}$$

A.5. Decision Variable

It is noted that $\alpha_{0,0}$ is a common factor of $Z_{PAM}^{(0)}$, M_{PAM}, I_{PAM} and N_{PAM}. Following auxiliary variables are defined by removing $\alpha_{0,0}$.

$$\begin{aligned}
\hat{Z}_{PAM}^{(0)} &= \alpha_{0,0} b_0^0 \sqrt{P} N_r \\
\hat{M}_{PAM}^{(k)} &= \sum_{l=0}^{L-1} \hat{M}_{PAM}^{(k,l)} = \sum_{l=0}^{L-1} \alpha_{k,l}\sqrt{P}\left[R_{PAM}(\Delta T_k) X_{PAM}^{(k,l)} + \hat{R}_{PAM}(\Delta T_k) Y_{PAM}^{(k,l)}\right] \\
\hat{M}_{PAM} &= \sum_{k=1}^{K-1} \hat{M}_{PAM}^{(k)} \\
\hat{I}_{PAM} &= \sum_{l=1}^{L-1} \hat{I}_{PAM}^{(l)} = \sqrt{P} \sum_{l=1}^{L-1} \alpha_{0,l} Y_{PAM}^{(0,l)} \\
\hat{N}_{PAM} &= \int_0^{T_r} n(t) \sum_{n=0}^{N_r-1} a_n^0 z(t - nT_c)dt
\end{aligned} \tag{18}$$

As proved in the Appendix, equivalent formulae (19) stand from the view point of statistical property. Hereafter, we will use the equivalent formulae.

$$\begin{aligned}
\hat{M}_{PAM}^{(k)} &= \sum_{l=0}^{L-1} \hat{M}_{PAM}^{(k,l)} = \sum_{l=0}^{L-1} \beta_{k,l}\sqrt{P}\left[R_{PAM}(\Delta T_k) X_{PAM}^{(k,l)} + \hat{R}_{PAM}(\Delta T_k) Y_{PAM}^{(k,l)}\right] \\
\hat{I}_{PAM} &= \sum_{l=1}^{L-1} \hat{I}_{PAM}^{(l)} = \sqrt{P} \sum_{l=1}^{L-1} \beta_{0,l} Y_{PAM}^{(0,l)}
\end{aligned} \tag{19}$$

Then Z_{PAM} is rewritten as

$$Z_{PAM} = \alpha_{0,0}(\hat{Z}_{PAM}^{(0)} + \hat{M}_{PAM} + \hat{I}_{PAM} + \hat{N}_{PAM}) \tag{20}$$

B. Characteristic Function Analysis

B.1. CF of MAI

It is observed in (19) that $\hat{M}_{PAM}^{(k)}$ consists of signals from L paths of the k^{th} user, where ΔT_k is a common factor. For a given ΔT_k, the values of $R_{PAM}(\Delta T_k)$ and $\hat{R}_{PAM}(\Delta T_k)$ are fixed, and L terms in the summation become independent. Characteristic function of $\hat{M}_{PAM}^{(k,l)}$ conditioned on ΔT_k and $\beta_{k,l}$, $\Phi_{\hat{M}_{PAM}^{(k,l)}|\Delta T_k,\beta_{k,l}}(\omega)$, is expressed as

$$\Phi_{\hat{M}_{PAM}^{(k,l)}|\Delta T_k,\beta_{k,l}}(\omega) = \left[\cos\left(\sqrt{P}R_{PAM}(\Delta T_k)\beta_{k,l}\omega\right)\cos\left(\sqrt{P}\hat{R}_{PAM}(\Delta T_k)\beta_{k,l}\omega\right)\right]^{N_r} \tag{21}$$

Characteristic function of $\hat{M}_{PAM}^{(k)}$ is given by

$$\Phi_{\hat{M}_{PAM}^{(k)}}(\omega) = \int_0^{Tc}\frac{1}{T_c}\left[\prod_{l=0}^{L-1}\int_0^{\infty}\Phi_{\hat{M}_{PAM}^{(k,l)}|\Delta T_k,\beta_{k,l}}(\omega)p_{\beta_{k,l}}(\beta_{k,l})d\beta_{k,l}\right]d\Delta T_k \tag{22}$$

where $p_{\beta_{k,l}}(\beta_{k,l})$ is PDF of channel fading amplitude $\beta_{k,l}$ in (3).

Since all users are mutually independent, $\Phi_{\hat{M}_{PAM}}(\omega)$ is a product of $\Phi_{\hat{M}_{PAM}^{(k)}}(\omega)$.

$$\Phi_{\hat{M}_{PAM}}(\omega) = \prod_{k=1}^{K-1}\Phi_{\hat{M}_{PAM}^{(k)}}(\omega) \tag{23}$$

B.2. CF of Self Interference

Characteristic function of $\hat{I}_{PAM}^{(l)}$ is given by

$$\Phi_{\hat{I}_{PAM}^{(l)}}(\omega) = \int_0^{\infty}\left[\cos(\sqrt{P}\beta_{0,l}\omega)\right]^{N_r}p_{\beta_{0,l}}(\beta_{0,l})d\beta_{0,l} \tag{24}$$

$\hat{I}_{PAM}$ is the sum of $L-1$ independent terms as shown in (19). Therefore $\Phi_{\hat{I}_{PAM}}(\omega)$ is given by

$$\Phi_{\hat{I}_{PAM}}(\omega) = \prod_{l=1}^{L-1}\Phi_{\hat{I}_{PAM}^{(l)}}(\omega) \tag{25}$$

B.3. CF of AWGN

$\hat{N}_{PAM}$ follows a Gaussian distribution with zero mean and variance of $N_0N_r/2$. Its characteristic function is given by [15]

$$\Phi_{\hat{N}_{PAM}}(\omega) = \exp(-\frac{N_0N_r\omega^2}{4}) \tag{26}$$

B.4. CF of Total Noise

As defined in (18), $\hat{M}_{PAM}^{(k)}$, $\hat{I}_{PAM}$ and $\hat{N}_{PAM}$ are statistically independent random variables. Characteristic function of their sum is calculated as

$$\Phi_{(\hat{M}_{PAM}+\hat{I}_{PAM}+\hat{N}_{PAM})}(\omega) = \Phi_{\hat{M}_{PAM}}(\omega)\Phi_{\hat{I}_{PAM}}(\omega)\Phi_{\hat{N}_{PAM}}(\omega) \tag{27}$$

IV. Characteristic Function Analysis of DS PPM UWB System

A. Decision Statistics

Output decision statistic Z_{PPM} is given by

$$\begin{aligned} Z_{PPM} &= \int_0^{T_r} r_{PPM}(t) v_{PPM}^{(0)}(t)dt \\ &= \underbrace{\int_0^{T_r} \alpha_{0,0} s_{PPM}^{(0)}(t) v_{PPM}^{(0)}(t)dt}_{Z_{PPM}^{(0)}} + \underbrace{\int_0^{T_r} \sum_{l=1}^{L-1} \alpha_{0,l} s_{PPM}^{(0)}(t-lT_c) v_{PPM}^{(0)}(t)dt}_{I_{PPM}} \\ &\quad + \underbrace{\int_0^{T_r} \sum_{k=1}^{K-1} \sum_{l=0}^{L-1} \alpha_{k,l} s_{PPM}^{(k)}(t-\tau_k-lT_c) v_{PPM}^{(0)}(t)dt}_{M_{PPM}} + \underbrace{\int_0^{T_r} n(t) v_{PPM}^{(0)}(t)dt}_{N_{PPM}} \end{aligned} \tag{28}$$

where $Z_{PPM}^{(0)}$ represents desired signal, I_{PPM} is SI due to multipath propagation, M_{PPM} stands for MAI, and N_{PPM} is the contribution of AWGN. Though Z_{PPM} shares a similar format with Z_{PAM}, different modulation method leads to different statistical property.

A.1. Desired Signal

$Z_{PPM}^{(0)}$ is given by

$$Z_{PPM}^{(0)} = \int_0^{T_r} \alpha_{0,0} s_{PPM}^{(0)}(t) \alpha_{0,0} \sum_{n=0}^{N_r-1} a_n^0 q(t-T_c)dt = \alpha_{0,0}^2(1-2b_0^0)\sqrt{P}N_r \tag{29}$$

A.2. Multiple Access Interference

M_{PPM} is expressed as

$$M_{PPM} = \sum_{k=1}^{K-1} \sum_{l=0}^{L-1} \underbrace{\int_0^{T_r} \alpha_{k,l} s_{PPM}^{(k)}(t-\tau_k-lT_c) \alpha_{0,0} \sum_{n=0}^{N_r-1} a_n^0 q(t-T_c)dt}_{M_{PPM}^{(k,l)}} \tag{30}$$

Interference from the l^{th} path of the k^{th} user, $M_{PPM}^{(k,l)}$, is modeled as

$$M_{PPM}^{(k,l)} = \begin{cases} \int_{\tau_{k,l}}^{T_r} \alpha_{k,l}\sqrt{P} \sum_{n=0}^{N_r-1} a_n^k z(t-\tau_{k,l}-nT_c-b_0^kT_p) v_{PPM}^{(0)}(t)dt & \text{if} \quad \tau_{k,l} < T_r \\ \int_0^{\tau_{k,l}-T_r} \alpha_{k,l}\sqrt{P} \sum_{n=0}^{N_r-1} a_n^k z(t-\tau_{k,l}+2T_r-nT_c-b_{-1}^kT_p) v_{PPM}^{(0)}(t)dt & \text{if} \quad \tau_{k,l} \geq T_r \end{cases} \tag{31}$$

To simplify $M_{PPM}^{(k,l)}$, following auxiliary definitions are introduced.

1) τ_k is split as an integer multiple of T_c and a remaining part ΔT_k.

$$\tau_k = \gamma_k T_c + \Delta T_k \tag{32}$$

where $\gamma_k \in \{0, 1, \cdots, N_r - 1\}$ and $\Delta T_k \in [0, T_c)$, both with uniform distribution.

2) $R_{PPM}(\Delta T_k, b_i^k)$ and $\hat{R}_{PPM}(\Delta T_k, b_i^k)$ are the cross correlation functions of $z(t)$ and $q(t)$. They are related with b_i^k, which may bring additional shift of monocycles.

$$\begin{aligned} R_{PPM}(\Delta T_k, b_i^k) &= \int_0^{\Delta T_k} q(t) z(t + T_c - \Delta T_k - b_i^k T_p) dt \\ \hat{R}_{PPM}(\Delta T_k, b_i^k) &= \int_{\Delta T_k}^{T_c} q(t) z(t - \Delta T_k - b_i^k T_p) dt \end{aligned} \tag{33}$$

3) $X_{PPM}(N)$ is defined as a Binomial random variable to represent the partial cross correlation of spreading codes of the desired user and the interfering user.

$$X_{PPM}(N) = \begin{cases} \sum_{n=1}^{N} c_n & N > 0 \\ 0 & \text{else} \end{cases} \tag{34}$$

where c_n takes value in $\{\pm 1\}$ with equal probability. The distribution of $X_{PPM}(N)$ is determined by N as given below

$$P(X_{PPM}(N) = x) = \begin{pmatrix} N \\ \frac{x+N}{2} \end{pmatrix} \frac{1}{2^N} \tag{35}$$

where the range of $X_{PPM}(N)$ is $\{-N, -N+2, \cdots, N-2, N\}$.

With the help of these auxiliary definitions, $M_{PPM}^{(k,l)}$ is rewritten as

$$M_{PPM}^{(k,l)} = \begin{cases} \alpha_{0,0}\alpha_{k,l}\sqrt{P}\Big[X_{PPM}(N_r - 1 - \gamma_k - l) R_{PPM}(\Delta T_k, b_0^k) \\ \qquad + X_{PPM}(N_r - \gamma_k - l) \hat{R}_{PPM}(\Delta T_k, b_0^k)\Big] & \text{if} \quad \tau_{k,l} < T_r \\ \alpha_{0,0}\alpha_{k,l}\sqrt{P}\Big[X_{PPM}(\gamma_k + l - N_r + 1) R_{PPM}(\Delta T_k, b_{-1}^k) \\ \qquad + X_{PPM}(\gamma_k + l - N_r) \hat{R}_{PPM}(\Delta T_k, b_{-1}^k)\Big] & \text{if} \quad \tau_{k,l} \geq T_r \end{cases} \tag{36}$$

Then $M_{PPM}^{(k,l)}$ is expressed as

$$M_{PPM}^{(k)} = \begin{cases} \alpha_{0,0}\sqrt{P}\Bigg[\sum_{l=0}^{L-1}\alpha_{k,l}X_{PPM}(N_r-1-\gamma_k-l)R_{PPM}(\Delta T_k, b_0^k) \\ \quad + \sum_{l=0}^{L-1}\alpha_{k,l}X_{PPM}(N_r-\gamma_k-l)\hat{R}_{PPM}(\Delta T_k, b_0^k)\Bigg] & \text{if} \quad \tau_{k,L-1} < T_r \\ \alpha_{0,0}\sqrt{P}\Bigg[\sum_{l=0}^{N_r-\gamma_k-1}\alpha_{k,l}X_{PPM}(N_r-1-\gamma_k-l)R_{PPM}(\Delta T_k, b_0^k) \\ \quad + \sum_{l=0}^{N_r-\gamma_k-1}\alpha_{k,l}X_{PPM}(N_r-\gamma_k-l)\hat{R}_{PPM}(\Delta T_k, b_0^k) \\ \quad + \sum_{l=N_r-\gamma_k}^{L-1}\alpha_{k,l}X_{PPM}(\gamma_k+l-N_r+1)R_{PPM}(\Delta T_k, b_{-1}^k) \\ \quad + \sum_{l=N_r-\gamma_k}^{L-1}\alpha_{k,l}X_{PPM}(\gamma_k+l-N_r)\hat{R}_{PPM}(\Delta T_k, b_{-1}^k)\Bigg] & \text{if} \quad \tau_{k,L-1} \geq T_r \end{cases} \tag{37}$$

A.3. Self Interference

Because of the guarding interval, there is no ISI. And SI comes from the current symbol b_0^0 only. SI from the l^{th} path, $I_{PPM}^{(l)}$ is modeled as

$$\begin{aligned} I_{PPM}^{(l)} &= \alpha_{0,0}\alpha_{0,l}\sqrt{P}\int_{lT_c}^{T_r}\sum_{m=0}^{N_r-1}a_m^0 z(t-lT_c-mT_c)\sum_{n=0}^{N_r-1}a_n^0 q(t-nT_c)dt \\ &= \alpha_{0,0}\alpha_{0,l}\sqrt{P}X_{PPM}(N_r-l)\hat{R}(0,b_0^0) \\ &= \alpha_{0,0}\alpha_{0,l}(1-2b_0^0)\sqrt{P}X_{PPM}(N_r-l) \end{aligned} \tag{38}$$

I_{PPM} is given by

$$I_{PPM} = \sum_{l=1}^{L-1} I_{PPM}^{(l)} = \alpha_{0,0}\sqrt{P}(1-2b_0^0)\sum_{l=1}^{L-1}\alpha_{0,l}X_{PPM}(N_r-l) \tag{39}$$

A.4. AWGN

N_{PPM} is obtained as

$$N_{PPM} = \alpha_{0,0}\int_0^{T_r} n(t)\sum_{n=0}^{N_r-1}a_n^0 q(t-nT_c)dt \tag{40}$$

A.5. Decision Variable

Similar to the DS PAM UWB system, $Z_{PPM}^{(0)}$, M_{PPM}, I_{PPM} and N_{PPM} contain a common factor $\alpha_{0,0}$. Following auxiliary variables are defined by removing $\alpha_{0,0}$. According to the proof in the Appendix, we substitute $\beta_{k,l}X_{PPM}(N)$ for $\alpha_{k,l}X_{PPM}(N)$ as an equivalent random variable.

$$\begin{aligned}
\hat{Z}_{PPM}^{(0)} &= \alpha_{0,0}(1-2b_0^0)\sqrt{P}N_r \\
\hat{M}_{PPM}^{(k,l)} &= \begin{cases} \beta_{k,l}\sqrt{P}[X_{PPM}(N_r-1-\gamma_k-l)R_{PPM}(\Delta T_k, b_0^k) & \\ \qquad +X_{PPM}(N_r-\gamma_k-l)\hat{R}_{PPM}(\Delta T_k, b_0^k)] & \text{if} \quad \tau_{k,l} < T_r \\ \beta_{k,l}\sqrt{P}[X_{PPM}(\gamma_k+l-N_r+1)R_{PPM}(\Delta T_k, b_{-1}^k) & \\ \qquad +X_{PPM}(\gamma_k+l-N_r)\hat{R}_{PPM}(\Delta T_k, b_{-1}^k)] & \text{if} \quad \tau_{k,l} \geq T_r \end{cases} \\
\hat{M}_{PPM} &= \sum_{k=1}^{K-1}\hat{M}_{PPM}^{(k)} = \sum_{k=1}^{K-1}\sum_{l=0}^{L-1}\hat{M}_{PPM}^{(k,l)} \\
\hat{I}_{PPM} &= \sum_{l=1}^{L-1}\hat{I}_{PPM}^{(l)} = \sqrt{P}(1-2b_0^0)\sum_{l=1}^{L-1}\beta_{0,l}X_{PPM}(N_r-l) \\
\hat{N}_{PPM} &= \int_0^{T_r} n(t)\sum_{n=0}^{N_r-1}a_n^0 q(t-nT_c)dt
\end{aligned} \tag{41}$$

Then Z_{PPM} is rewritten as

$$Z_{PPM} = \alpha_{0,0}(\hat{Z}_{PPM}^{(0)} + \hat{M}_{PPM} + \hat{I}_{PPM} + \hat{N}_{PPM}) \tag{42}$$

B. Characteristic Function Analysis

B.1. CF of MAI

For given γ_k, ΔT_k, b_{-1}^k and b_0^k, characteristic function of $\hat{M}_{PPM}^{(k,l)}$ is given by

$$\Phi_{\hat{M}_{PPM}^{(k,l)}|\gamma_k,\Delta T_k,b_{-1}^k,b_0^k}(\omega) = \begin{cases} \int_0^\infty \left[\cos\left(\beta_{k,l}\sqrt{P}R_{PPM}(\Delta T_k, b_0^k)\omega\right)\right]^{N_r-1-\gamma_k-l} & \\ \quad \cdot\left[\cos\left(\beta_{k,l}\sqrt{P}\hat{R}_{PPM}(\Delta T_k, b_0^k)\omega\right)\right]^{N_r-\gamma_k-l} & \\ \quad \cdot p_{\beta_{k,l}}(\beta_{k,l})d\beta_{k,l} & \text{if} \quad \tau_{k,l} < T_r \\ \int_0^\infty \left[\cos\left(\beta_{k,l}\sqrt{P}R_{PPM}(\Delta T_k, b_{-1}^k)\omega\right)\right]^{\gamma_k+l-N_r+1} & \\ \quad \cdot\left[\cos\left(\beta_{k,l}\sqrt{P}\hat{R}_{PPM}(\Delta T_k, b_{-1}^k)\omega\right)\right]^{\gamma_k+l-N_r} & \\ \quad \cdot p_{\beta_{k,l}}(\beta_{k,l})d\beta_{k,l} & \text{if} \quad \tau_{k,l} \geq T_r \end{cases} \tag{43}$$

For different l, $\hat{M}_{PPM}^{(k,l)}$ conditioned on γ_k, ΔT_k, b_{-1}^k and b_0^k are independent. Thus conditional characteristic function of $\hat{M}_{PPM}^{(k)}$ is expressed in a product form.

$$\Phi_{\hat{M}_{PPM}^{(k)}|\gamma_k,\Delta T_k,b_{-1}^k,b_0^k}(\omega) = \prod_{l=0}^{L-1} \Phi_{\hat{M}_{PPM}^{(k,l)}|\gamma_k,\Delta T_k,b_{-1}^k,b_0^k}(\omega) \tag{44}$$

$\Phi_{\hat{M}_{PPM}^{(k)}}(\omega)$ is obtained by averaging over PDF of all conditional variables.

$$\begin{aligned}\Phi_{\hat{M}_{PPM}^{(k)}}(\omega) &= \frac{1}{4N_rT_c}\sum_{\gamma_k=0}^{N_r-1}\int_0^{T_c} \Phi_{\hat{M}_{PPM}^{(k)}|\gamma_k,\Delta T_k,0,0}(\omega) + \Phi_{\hat{M}_{PPM}^{(k)}|\gamma_k,\Delta T_k,0,1}(\omega) \\ &\qquad + \Phi_{\hat{M}_{PPM}^{(k)}|\gamma_k,\Delta T_k,1,0}(\omega) + \Phi_{\hat{M}_{PPM}^{(k)}|\gamma_k,\Delta T_k,1,1}(\omega) d\Delta T_k \end{aligned}\tag{45}$$

Due to independence of all users, $\Phi_{\hat{M}_{PPM}}(\omega)$ is given as follows.

$$\Phi_{\hat{M}_{PPM}}(\omega) = \prod_{k=1}^{K-1} \Phi_{\hat{M}_{PPM}^{(k)}}(\omega) \tag{46}$$

B.2. CF of Self Interference

$\hat{I}_{PPM}$ comes from the 1^{st} to the $L-1^{th}$ paths of the desired user. And characteristic function of $\hat{I}_{PPM}^{(l)}$ is given by

$$\begin{aligned}\Phi_{\hat{I}_{PPM}^{(l)}}(\omega) &= \int_0^\infty \left[\cos(\sqrt{P}(1-2b_0^0)\beta_{0,l}\omega)\right]^{N_r-l} p_{\beta_{0,l}}(\beta_{0,l})d\beta_{0,l} \\ &= \int_0^\infty \left[\cos(\sqrt{P}\beta_{0,l}\omega)\right]^{N_r-l} p_{\beta_{0,l}}(\beta_{0,l})d\beta_{0,l}\end{aligned}\tag{47}$$

The characteristic function of $\hat{I}_{PPM}$ is obtained as follows.

$$\Phi_{\hat{I}_{PPM}}(\omega) = \prod_{l=1}^{L-1} \Phi_{\hat{I}_{PPM}^{(l)}}(\omega) \tag{48}$$

B.3. CF of AWGN

$\hat{N}_{PPM}$ follows a Gaussian distribution with zero mean and variance of N_0N_r. Its characteristic function $\Phi_{\hat{N}_{PPM}}$ is given by [16]

$$\Phi_{\hat{N}_{PPM}}(\omega) = \exp(-\frac{N_0N_r\omega^2}{2}) \tag{49}$$

B.4. CF of Total Noise

Since $\hat{M}_{PPM}$, $\hat{I}_{PPM}$ and $\hat{N}_{PPM}$ are independent random variables, characteristic function of their sum is expressed as below.

$$\Phi_{(\hat{M}_{PPM}+\hat{I}_{PPM}+\hat{N}_{PPM})}(\omega) = \Phi_{\hat{M}_{PPM}}(\omega)\Phi_{\hat{I}_{PPM}}(\omega)\Phi_{\hat{N}_{PPM}}(\omega) \tag{50}$$

V. Bit Error Rate Formula

Characteristic function of the total noise, $\hat{\varsigma}_{PAM/PPM} = \hat{M}_{PAM/PPM} + \hat{I}_{PAM/PPM} + \hat{N}_{PAM/PPM}$, is derived in the previous sections. PDF of $\hat{\varsigma}_{PAM/PPM}$ is obtained by performing an inverse Fourier transform on (27) and (50).

$$p_{\hat{\varsigma}_{PAM/PPM}}(x) = \frac{1}{2\pi}\int_{-\infty}^{\infty} \Phi_{\hat{\varsigma}_{PAM/PPM}}(\omega)\exp(-j\omega x)d\omega \tag{51}$$

The decision rule of the DS UWB systems is given by

$$\begin{cases} Z_{PAM/PPM} > 0 \Rightarrow b_0^0 = 1/0 \\ Z_{PAM/PPM} \leq 0 \Rightarrow b_0^0 = -1/1 \end{cases} \tag{52}$$

The BER formula is obtained by two fold integrations as below.

$$\begin{aligned} P_{\text{Average}} &= \frac{1}{2}\text{Prob}(Z_{PAM/PPM} \leq 0|b_0^0 = 1/0) + \frac{1}{2}\text{Prob}(Z_{PAM/PPM} > 0|b_0^0 = -1/1) \\ &= \text{Prob}\left(\alpha_{0,0}(\alpha_{0,0}\sqrt{P}N_r + \hat{\varsigma}_{PAM/PPM}) \leq 0\right) \\ &= \text{Prob}\left(\hat{\varsigma}_{PAM/PPM} \leq -\beta_{0,0}\sqrt{P}N_r\right) \\ &= \int_0^{\infty}\int_{-\infty}^{-\beta_{0,0}\sqrt{P}N_r} p_{\hat{\varsigma}_{PAM/PPM}}(x)dx p_{\beta_{0,0}}(\beta_{0,0})d\beta_{0,0} \\ &= \frac{1}{2} - \frac{1}{\pi}\int_0^{\infty}\int_0^{\infty}\Phi_{\hat{\varsigma}_{PAM/PPM}}(\omega)\frac{\sin(\beta_{0,0}\sqrt{P}N_r\omega)}{\omega}d\omega p_{\beta_{0,0}}(\beta_{0,0})d\beta_{0,0} \end{aligned} \tag{53}$$

Though the integration range about ω and $\beta_{0,0}$ in (53) is infinity, it can be safely truncated to finite range in numerical computation. The reason is that both $\frac{\sin(\beta_{0,0}\sqrt{P}N_r\omega)}{\omega}$ and $p_{\beta_{0,0}}(\beta_{0,0})$ have fast decaying tails. As shown in (53), P_{Average} is a function of $p_{\beta_{k,l}}(\beta_{k,l})$. As suggested in [17], $p_{\beta_{k,l}}(\beta_{k,l})$ takes the form in (3). Yet $p_{\beta_{k,l}}(\beta_{k,l})$ can also take other forms. Therefore the analytical method is applicable to arbitrary multipath fading channels.

VI. BER Derivation Using GA Method

For completeness and comparison, BER calculation using the GA method is briefly described. The total noise $\hat{\varsigma}_{PAM/PPM}$ is assumed to be Gaussian distributed. Since $\hat{M}_{PAM/PPM}$, $\hat{I}_{PAM/PPM}$ and $\hat{N}_{PAM/PPM}$ are statistically independent, the variance of $\hat{\varsigma}_{PAM/PPM}$ is given by

$$\begin{aligned} \sigma^2_{\hat{\varsigma}_{PAM/PPM}} &= \sigma^2_{\hat{M}_{PAM/PPM}} + \sigma^2_{\hat{I}_{PAM/PPM}} + \sigma^2_{\hat{N}_{PAM/PPM}} \\ &= \sum_{k=1}^{K-1} \sigma^2_{\hat{M}^{(k)}_{PAM/PPM}} + \sigma^2_{\hat{I}_{PAM/PPM}} + \sigma^2_{\hat{N}_{PAM/PPM}} \end{aligned} \tag{54}$$

where $\sigma^2_{\hat{N}_{PAM}} = \frac{N_0 N_r}{2}$, $\sigma^2_{\hat{N}_{PPM}} = N_0 N_r$ and

$$\begin{aligned} \sigma^2_{\hat{M}^{(k)}_{PAM/PPM}} &= E\left[(\hat{M}^{(k)}_{PAM/PPM})^2\right] = \sum_{l=0}^{L-1} E\left[(\hat{M}^{(k,l)}_{PAM/PPM})^2\right] \\ \sigma^2_{\hat{I}_{PAM/PPM}} &= E\left[(\hat{I}_{PAM/PPM})^2\right] = \sum_{l=1}^{L-1} E\left[(\hat{I}^{(l)}_{PAM/PPM})^2\right] \end{aligned} \tag{55}$$

Instantaneous BER is given by the following expression.

$$P_{\text{Instant}} = \frac{1}{2}\text{erfc}\left(\sqrt{\frac{\gamma_{PAM/PPM}}{2}}\right) \tag{56}$$

where $\gamma_{PAM/PPM}$ is instantaneous output SINR defined by

$$\gamma_{PAM/PPM} = \frac{(\hat{Z}^{(0)}_{PAM/PPM})^2}{\sigma^2_{\hat{\varsigma}_{PAM/PPM}}} = \frac{\alpha^2_{0,0} P N_r^2}{\sigma^2_{\hat{\varsigma}_{PAM/PPM}}} \tag{57}$$

Average BER is obtained by

$$P_{\text{Average}} = \int_0^\infty P_{\text{Instant}}(\gamma) p_{\gamma_{PAM/PPM}}(\gamma) d\gamma \tag{58}$$

where $p_{\gamma_{PAM/PPM}}(\gamma)$ is PDF of the instantaneous SINR. Average BER in lognormal multipath fading channels is computed using Monte Carlo method.

VII. Numerical Results and Comparison

A commonly used Gaussian monocycle $z(t)$ is adopted in the numerical study. Nevertheless, the analysis in this work is applicable for any UWB monocycle waveform.

$$z(t) = A \exp\left[-0.5\left(\frac{t}{\sigma} - 3.5\right)^2\right] \tag{59}$$

where duration of $z(t)$ is $T_p = 0.25$ns, the time normalization factor $\sigma = T_p/7 \approx 0.035714$ns, the energy normalization factor $A = 1.25687 \times 10^5$. Transmitted power of all users is assumed to be P. Transmitted energy of one symbol (including N_r monocycles) is $E_b = PN_r$. Though average received power of all users is the same, channel fading leads to random instantaneous received power. Other system parameters are set as $T_c = 1$ns, $N_r = 512, 1024$. Channel parameters are listed in Table I according to [17].

The autocorrelation function of $z(t)$ defined in (11), $\hat{R}_{PAM}(x)$, has a closed form as given in (60). In Fig. 1, $R_{PAM}(\Delta T_k)$ and $\hat{R}_{PAM}(\Delta T_k)$ are plotted. The cross correlation function of $z(t)$ and $q(t)$ defined in (33), $R_{PPM}(\Delta T_k, b_i^k)$ and $\hat{R}_{PPM}(\Delta T_k, b_i^k)$, are plotted in Fig. 2.

$$\hat{R}_{PAM}(x) = \frac{T_c\sqrt{\pi}A^2}{56} \exp\left(-\left(\frac{x}{2\sigma}\right)^2\right) \operatorname{erfc}\left(\sqrt{2}\left(\frac{x}{\sigma} - 3.5\right) - \frac{x}{\sqrt{2}\sigma}\right) \tag{60}$$

In Fig. 3 and Fig. 4, comparison of accuracy of the CF and GA methods is shown for $N_r = 512$ and 1024 respectively. Theoretical BER curves generated by the CF method (solid line) and the GA method (dashed line) are plotted along with simulation results (circle marked). In these two figures, theoretical BER curves generated by the CF method exactly match with the corresponding simulation results. The GA theoretical BER curves are in good agreement with simulation results for small SNR values. However, the GA method is not as accurate in high SNR range (around 15dB and above). In small SNR range, AWGN dominates the total noise. Hence, the total noise can be approximated as Gaussian distributed. However, in high SNR range, MAI and SI have more important impact on total noise. Since MAI and SI generally does not follow Gaussian distribution in a fading environment, the GA method does not work well in high SNR range. In Fig. 6 and Fig. 7, characteristic function of each term is plotted for a fixed high SNR of $E_b/N_0 = 35$dB. It is observed that $\Phi_{\text{TotalNoise}}$ is under the influence of MAI and SI, which is apparently different from Φ_{AWGN}.

In Fig. 5, multiple access performance of these two systems is compared in case of large number of users. With the growth of number of users, BER performance degrades as expected. Multiple access performance of the DS PAM UWB system is slightly better than the DS PPM UWB system. As shown in Fig. 3 and Fig. 4, the DS PAM UWB system also outperforms the DS PPM UWB system. Similar results were reported for comparison of TH PSK UWB and TH PPM UWB systems in AWGN channels [19].

The characteristic functions of MAI, SI and AWGN are plotted in Fig. 6 and Fig. 7, which provide further insight into performance comparison of the DS PAM UWB and DS PPM UWB systems. It is found that $\Phi_{\text{TotalNoise}}$ in the DS PPM UWB system is more peaked than $\Phi_{\text{TotalNoise}}$ in the DS PAM UWB system. This implies that PDF of the total noise in the DS PPM UWB system would be flatter than that of the DS PAM UWB system. Since average BER is obtained by a tail integration on PDF of the total noise, BER performance of the DS PPM UWB system would worse than that of the DS PAM UWB system.

VIII. Conclusions

Exact BER formula of the DS PAM UWB and DS PPM UWB multiple access systems is derived using the CF method in lognormal multipath fading channels. Instead of approximating interference as Gaussian distributed, the relationship between the PDF and the characteristic function is utilized to find the distribution of total noise. Thereafter average BER values are computed based on exact PDF of the total noise. Our study shows that more accurate BER evaluation can be obtained by the CF method. Then performance comparison based on the BER formula indicates actual performance difference of the DS PAM UWB and DS PPM UWB systems. The characteristic function and distribution analysis of interference in DS UWB systems also provides the theoretical basis for further study on interference suppression.

Appendix

In (12) and (34), three Binomial random variables, $X_{PAM}^{(k,l)}$, $Y_{PAM}^{(k,l)}$ and $X_{PPM}(N)$, are defined. Their distributions are given in (13) and (35) respectively. It can be proved that the distribution of $\alpha_{k,l}X$

is the same as that of $\beta_{k,l}X$, where X denotes any one of $X_{PAM}^{(k,l)}$, $Y_{PAM}^{(k,l)}$ and $X_{PPM}(N)$.

Recall that $\alpha_{k,l}X = \theta_{k,l}\beta_{k,l}X$. Hence we only need to prove distribution of $\theta_{k,l}X$ is the same as that of X. The proof for $\theta_{k,l}X_{PAM}^{(k,l)}$ is given below, and the other two can be proved similarly.

$$\begin{aligned} P\left(\theta_{k,l}X_{PAM}^{(k,l)} = x\right) &= \frac{1}{2}P\left(X_{PAM}^{(k,l)} = x\right) + \frac{1}{2}P\left(-X_{PAM}^{(k,l)} = x\right) \\ &= \frac{1}{2^{N_r+1}}\begin{pmatrix} N_r \\ \frac{N_r+x}{2} \end{pmatrix} + \frac{1}{2^{N_r+1}}\begin{pmatrix} N_r \\ \frac{N_r-x}{2} \end{pmatrix} \\ &= \frac{1}{2^{N_r}}\begin{pmatrix} N_r \\ \frac{N_r+x}{2} \end{pmatrix} \\ &= P\left(X_{PAM}^{(k,l)} = x\right) \end{aligned} \tag{61}$$

References

[1] M. Z. Win and R. A. Scholtz, "Ultra-wide bandwidth time-hopping spread-spectrum impulse radio for wireless multiple-access communications," *IEEE Trans. Commun*, vol. 48, no. 4, pp. 679–689, Apr 2000.

[2] N. Boubaker and K. B. Letaief, "Ultra wideband DSSS for multiple access communications using antipodal signaling," in *IEEE International Conference on Communications*, May 2003, pp. 2197–2201.

[3] B. R. Vojcic and R. L. Pickholtz, "Direct-sequence code division multiple access for ultra-wide bandwidth impulse radio," in *Proc of Milcom 2003*, Oct 2003, pp. 898–902.

[4] P. Runkle, J. McCorkle, T. Miller, and M. Welborn, "DS-CDMA: the modulation technology of choice for UWB communications," in *2003 IEEE Conference on Ultra Wideband Systems and Technologies*, Nov 2003, pp. 364–368.

[5] L. Piazzo, "Performance analysis and optimization for impulse radio and direct-sequence impulse radio in multiuser interference," *IEEE Transaction on Communications*, vol. 52, no. 5, pp. 801–810, May 2004.

[6] H. Liu, "Error performance of a pulse amplitude and position modulated ultra-wideband system over lognormal fading channels," *IEEE Communications Letters*, vol. 7, no. 11, pp. 531–533, Nov 2003.

[7] D. C. Laney, G. M. Maggio, F. Lehmann, and L. Larson, "Multiple access for UWB impulse radio with pseudochaotic time hopping," *Selected Areas in Communications, IEEE Journal on*, vol. 20, no. 9, pp. 1692–1700, Dec 2002.

[8] H. R. Ahmadi and M. Nasiri-Kenar, "Performance analysis of time-hopping ultra-wideband systems in multipath fading channels (uncoded and coded schemes)," in *Personal, Indoor and Mobile Radio Communications, 2002. The 13th IEEE International Symposium on*, vol. 4, Sep 2002, pp. 1694–1698.

[9] B. Hu and N. C. Beaulieu, "Accurate evaluation of multiple-access performance in TH-PPM and TH-BPSK UWB systems," *IEEE Transactions on Communications*, vol. 52, no. 10, pp. 1758–1766, Oct 2004.

[10] N. Boubaker and K. B. Letaief, "Performance analysis of DS-UWB multiple access under imperfect power control," *IEEE Trans. Commun.*, vol. 52, no. 9, pp. 1459–1463, Sep 2004.

[11] J. R. Foerster, "The performance of a direct-sequence spread ultra-wideband system in the presence of multipath, narrowband interference, and multiuser interference," in *IEEE Conference on Ultra Wideband Systems and Technologies*, May 2002, pp. 87–91.

[12] V. Venkatesan, H. Liu, C. Nilsen, R. Kyker, and M. E. Magana, "Performance of an optimally spaced PPM ultra-wideband system with direct sequence spreading for multiple access," in *Proc of IEEE VTC 2003-Fall*, Oct 2003, pp. 602–606.

[13] V. S. Somayazulu, "Multiple access performance in UWB systems using time hopping vs. direct sequence spreading," in *Proc of IEEE WCNC*, Mar 2002, pp. 522–525.

[14] G. Durisi and G. Romano, "On the validity of gaussian approximation to characterize the multiuser capacity of UWB TH PPM," in *IEEE Conference on Ultra Wideband Systems and Technologies*, May 2002, pp. 157–161.

[15] W. Cao, A. Nallanathan, B. Kannan, and C. C. Chai, "Exact BER analysis of DS-UWB multiple access system under imperfect power control," in *Proc of IEEE VTC 2005-Fall*, Sep 2005, pp. 986–990.

[16] ——, "Exact BER analysis of DS PPM UWB multiple access system under imperfect power control," in *Proc of MILCOM 2005*, Oct 2005, pp. 1–6.

[17] J. R. Foerster, "Channel modeling sub-committee report final (doc: IEEE 802-15-02/490r1-sg3a)," Feb 2002.

[18] A. Papoulis and S. U. Pillai, *Probability, random variables and stochastic processes*, p. 93, 2002.

[19] G. Durisi and S. Benedetto, "Performance evaluation and comparison of different modulation schemes for UWB multiaccess systems," in *IEEE ICC 2003*, May 2003, pp. 2187–2191.

TABLE I

THE PARAMETERS USED IN NUMERICAL STUDY

Model Parameters	CM1
Γ_1 (cluster power decay factor)	7.1
Γ_2 (ray power decay factor)	4.3
σ_1 (stand. dev. of cluster lognormal fading term in dB)	3.3941
σ_2 (stand. dev. of ray lognormal fading term in dB)	3.3941
L (path number)	12

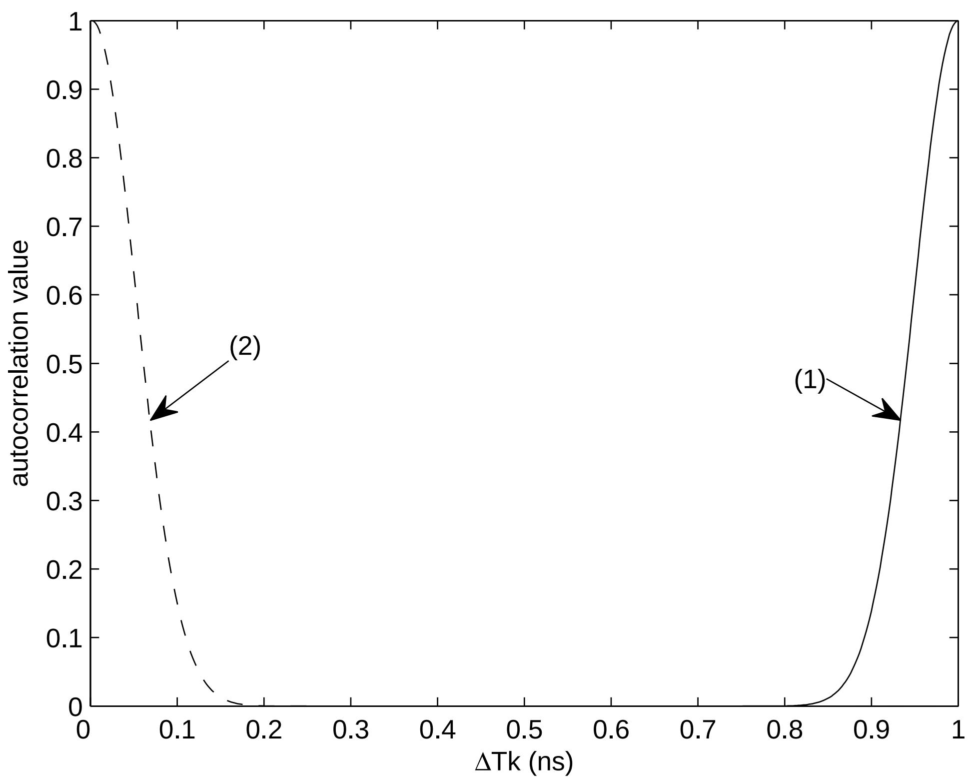

Fig. 1. The autocorrelation functions of $z(t)$: (1) is $R_{PAM}(\Delta T_k)$, (2) is $\hat{R}_{PAM}(\Delta T_k)$.

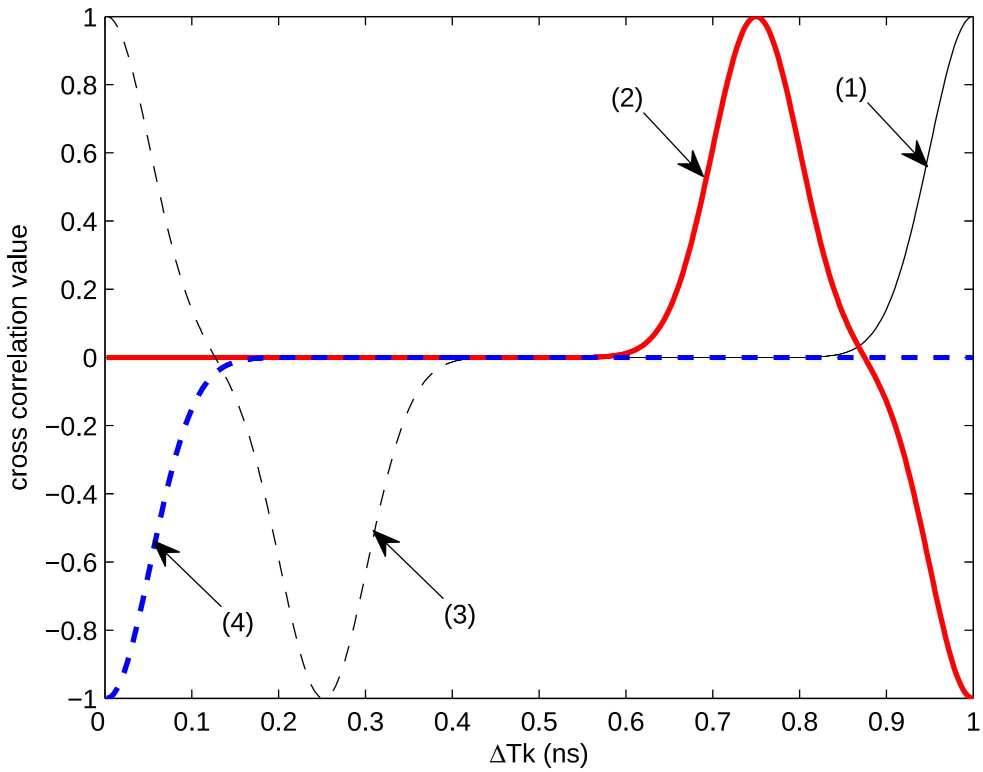

Fig. 2. The cross correlation functions of $z(t)$ and $q(t)$: (1) is $R_{PPM}(\Delta T_k, 0)$, (2) is $R_{PPM}(\Delta T_k, 1)$, (3) is $\hat{R}_{PPM}(\Delta T_k, 0)$, (4) is $\hat{R}_{PPM}(\Delta T_k, 1)$.

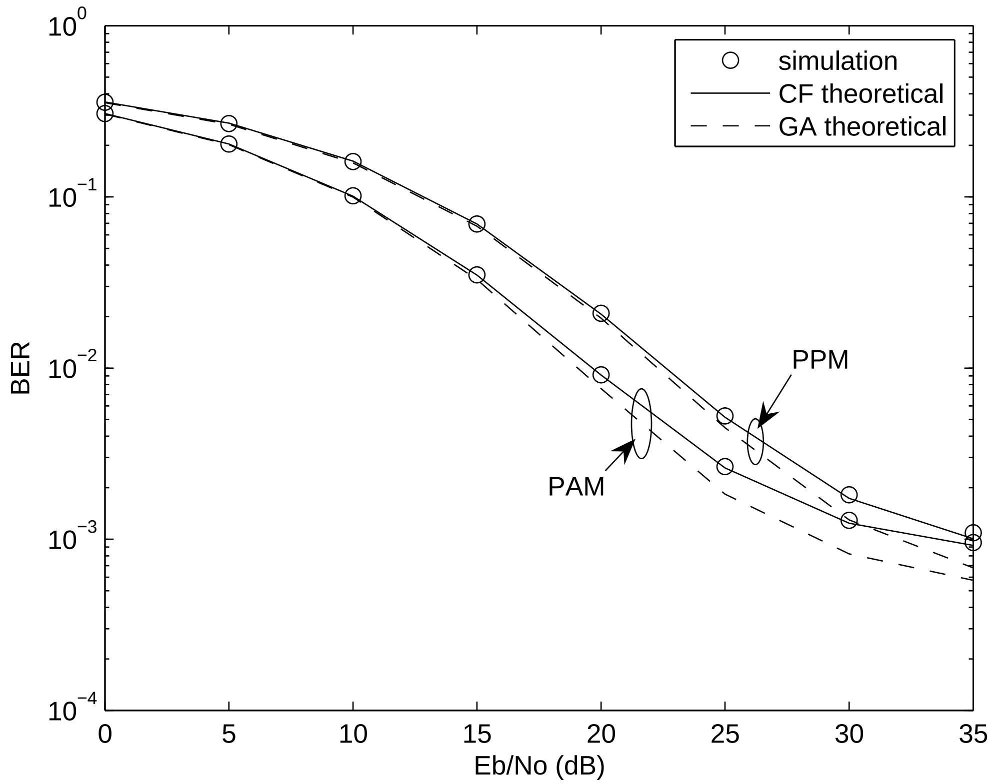

Fig. 3. Comparison of the CF and GA methods, $N_r = 512$, $K = 2$.

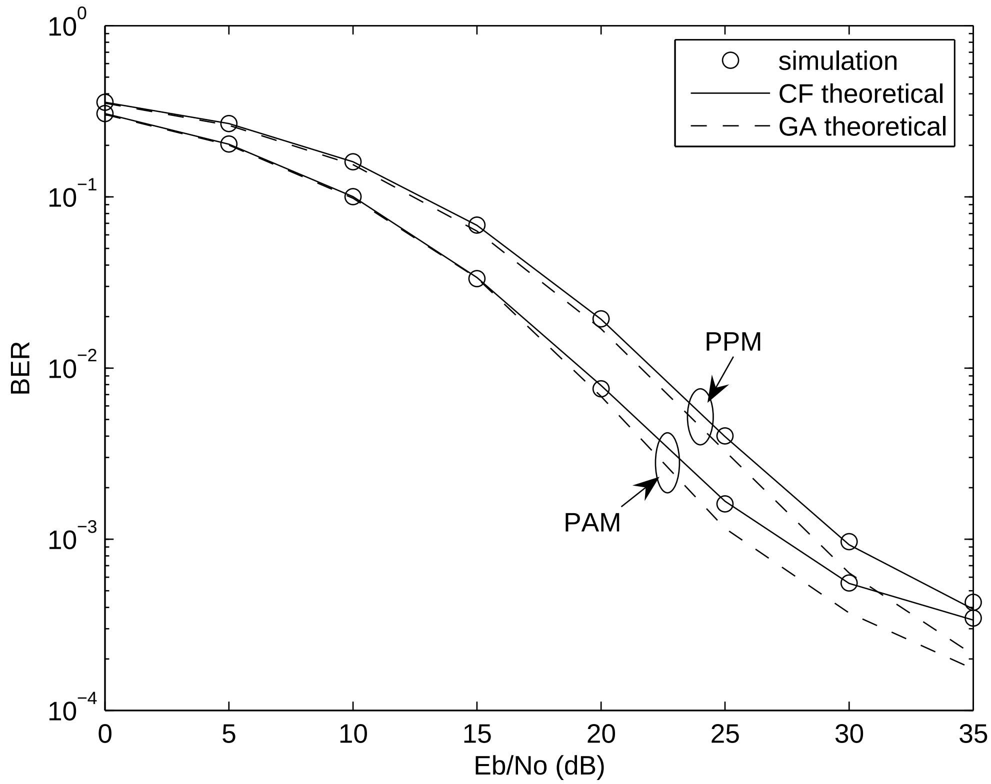

Fig. 4. Comparison of the CF and GA methods, $N_r = 1024$, $K = 4$.

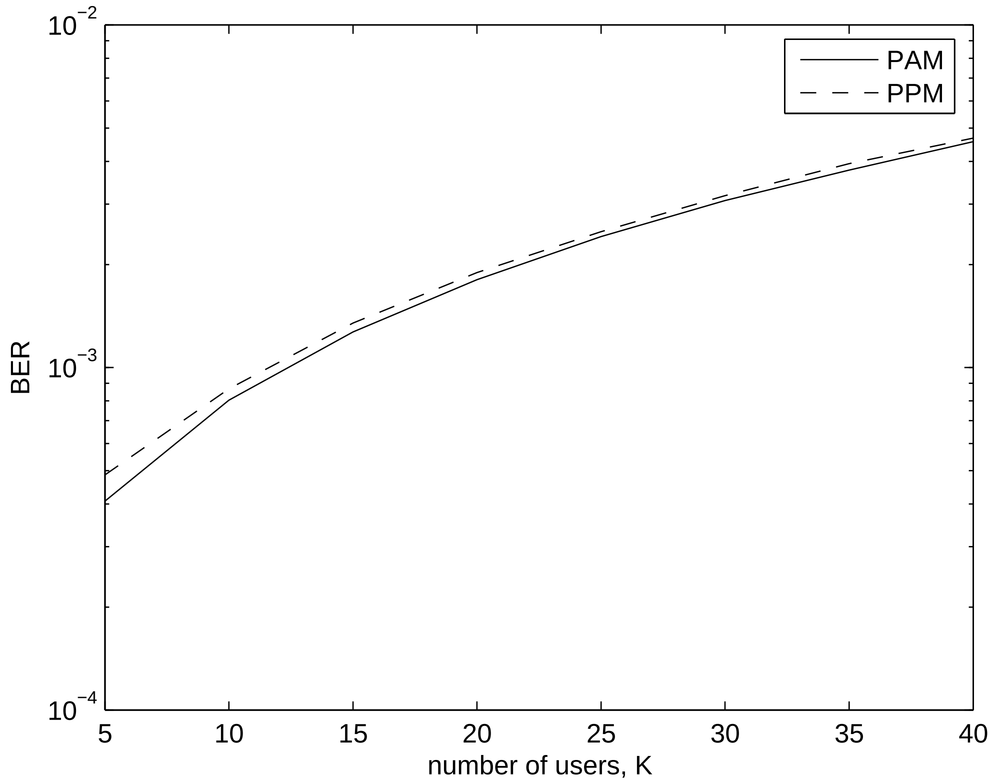

Fig. 5. BER performance with different number of users, $N_r = 1024$, $E_b/N_0 = 35$dB.

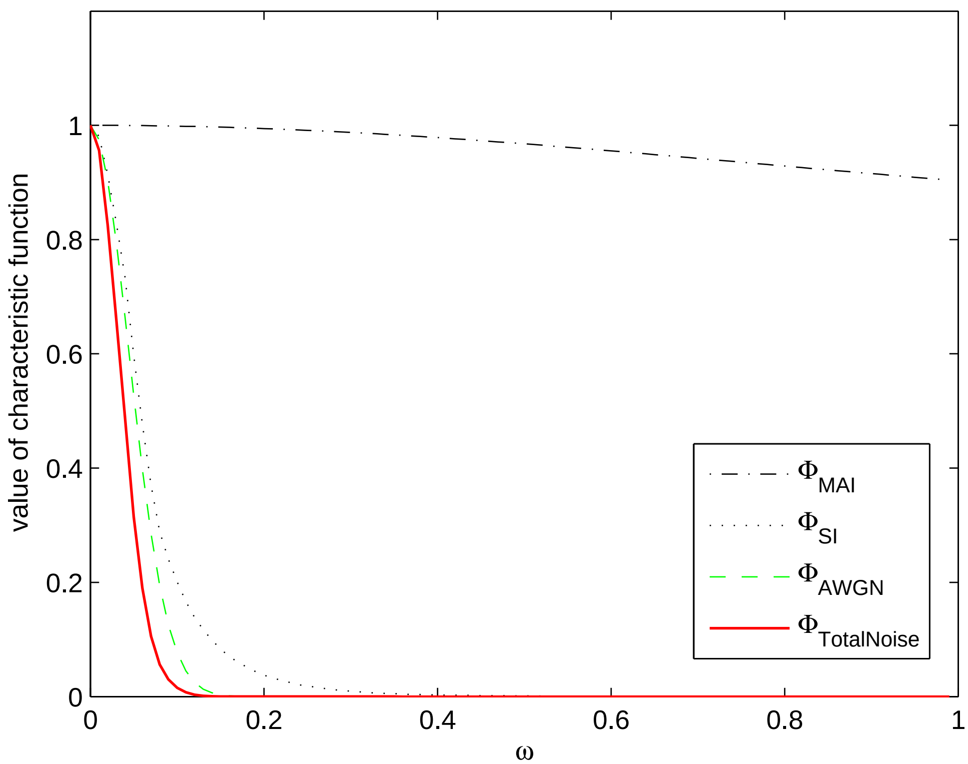

Fig. 6. Characteristic functions of the DS PAM UWB system, $N_r = 512$, $K = 2$, $E_b/N_0 = 35$dB.

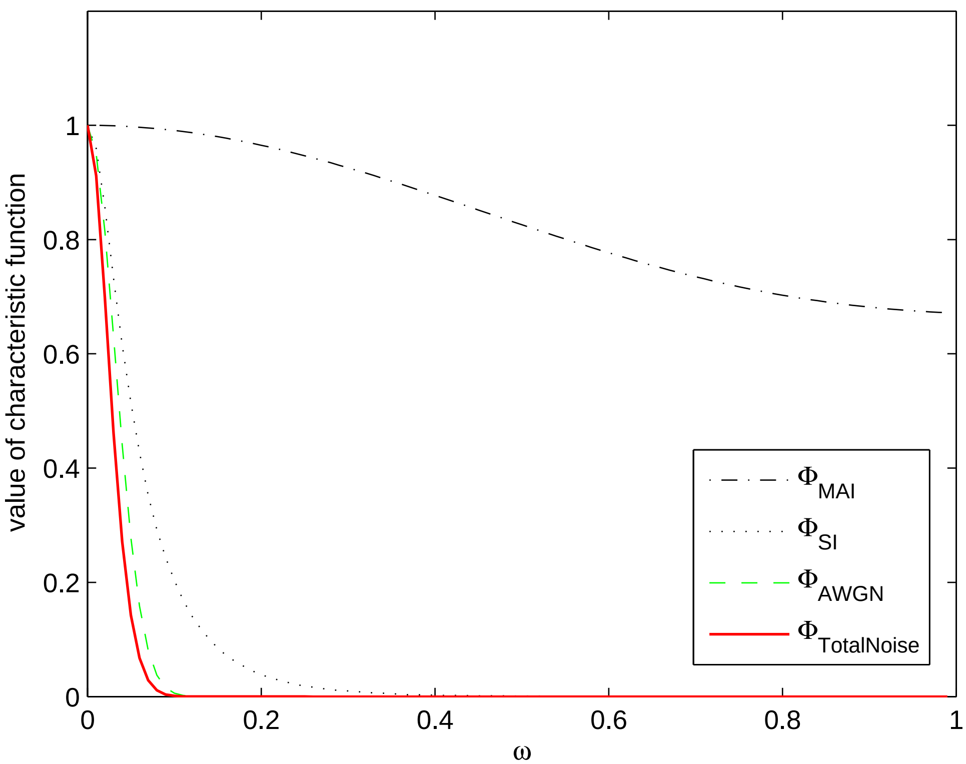

Fig. 7. Characteristic functions of the DS PPM UWB system, $N_r = 512$, $K = 2$, $E_b/N_0 = 35$dB.